JAIST Repository
https://dspace.jaist.ac.jp/

Title	Effect of Molecular Orientation to Proton Conductivity in Sulfonated Polyimides with bent backbones
Author(s)	Nagao, Yuki; Ohno, Kazuki; Tsuyuki, Shinya; Suetsugu, Kota; Hara, Mitsuo; Nagano, Shusaku
Citation	Molecular Crystals and Liquid Crystals, 686(1): 84-91
Issue Date	2019-10-10
Type	Journal Article
Text version	author
URL	http://hdl.handle.net/10119/16897
Rights	This is an Author's Accepted Manuscript of an article published in Molecular Crystals and Liquid Crystals, 686(1), 2019, pp.84-91. Copyright (C) 2019 Taylor & Francis, available online at: https://doi.org/10.1080/15421406.2019.1648041
Description	

JAIST
JAPAN
ADVANCED INSTITUTE OF
SCIENCE AND TECHNOLOGY

Japan Advanced Institute of Science and Technology

Effect of Molecular Orientation to Proton Conductivity in Sulfonated Polyimides with bent backbones

Yuki Nagao[a,*], Kazuki Ohno[a], Shinya Tsuyuki[a], Kota Suetsugu[b], Mitsuo Hara[b], Shusaku Nagano[c]

[a]School of Materials Science, Japan Advanced Institute of Science and Technology, 1-1 Asahidai, Nomi, Ishikawa 923-1292, Japan

[b]Department of Molecular Design & Engineering Graduate School of Engineering, Nagoya University, Furo-cho, Chikusa, Nagoya 464-8603, Japan

[c]Nagoya University Venture Business Laboratory, Nagoya University, Furo-cho, Chikusa, Nagoya 464-8603, Japan

Corresponding Author

*(Y.N.) E-mail: ynagao@jaist.ac.jp. Telephone: +81(Japan)-761-51-1541. Fax: +81(Japan)-761-51-1149

Running Head :

Effect of Molecular Orientation to Proton Conductivity in Sulfonated Polyimides

ABSTRACT

Two organized sulfonated polyimides (ASPIs) with bent polymer backbones were synthesized to study a relation between structure and proton conductivity. Proton conductivity exhibited different values between the thin film and bulk pelletized forms. Results from small-angle X-ray scattering (SAXS) and attenuated total reflection measurements suggest that the orientation of backbones is different between the thin film and bulk forms. SAXS results suggest excess amount of water uptake in the bulk samples compared to the thin film form. These structure and water uptake property could contribute the difference of the proton conductivity between the thin film and bulk pelletized forms.

Keywords : Sulfonated polyimide, Molecular orientation, In-plane orientation, Organized structure, Proton conductivity, Lyotropic liquid crystalline property

Introduction

Research on constructing ion conducting channels based on a hierarchical structure by organizing molecules and polymers has been attracting attention. A Nafion membrane,[1-2] which is well known as a high proton conductive polymer, has a phase segregated structure by hydrophilic side chain and hydrophobic backbone. Because of the less molecular ordering nature of Nafion, controlling the polymer structure is not easy work to enhance the property and reduce the production cost. From this background, an organized structure, which enables X-ray scattering techniques for discussing the structure, has attracted attention for the development of the highly proton-conductive polymers.[3]

From the viewpoint of structural control, functional design based on liquid crystalline (LC) property that spontaneously forms periodic molecular aggregates could give high proton transport property through a formation of self-assembled transport channels because of intermolecular interaction such as hydrophilic and hydrophobic interactions. Kato and co-workers demonstrated ion-transport pathways by the LC property. [4-6] In recent years, studies on the organized structure and ionic conductivity in various LC phases have been reported by thermotropic and lyotropic LC property. [7-10] Matsui and co-workers demonstrated a 2D high proton conduction in multi-lamellar organized structure by a Langmuir–Blodgett technique. [11-13]。

The first highly proton-conductive thin films with the organized structure have been reported by Nagao and coworkers in 2014.[14] The thin film of the alkyl sulfonated polyimide (ASPI) exhibits an organized lamellar structure by water uptake. The polymer backbone oriented parallel to the substrate surface (in-plane orientation). The lamellar distance can reversibly vary by the

amount of water uptake. The degree of the molecular ordering was also improved by water uptake. This reversible structural change occurs by the lyotropic LC property. The formed water nano-channel in the lamellar organized structure contributes to high proton conductivity of 10^{-1} S cm^{-1}. Some ASPI thin films have been synthesized and investigated for the relation between the organized structure and proton conductivity.[14-19] Compared to the planar and bent polymer backbones in ASPI thin films, ASPI-1 and ASPI-2 thin films with a planar backbone exhibit the higher proton conductivity.[18] And proton conductivity of the thin film was higher than that of the bulk pelletized sample because of the difference of the degree of in-plane orientation of the polymer backbone.[14] However, there is no discussion for the relation between the polymer orientation and proton conductivity in the bulk pelletized samples with bent backbone structure. In this study, two ASPI-3 and ASPI-4 with bent backbones as shown in Scheme 1 were synthesized and studied on the proton conductivity and polymer structure by impedance spectroscopy, small-angle X-ray scattering (SAXS), and attenuated total reflection (ATR) measurements.

Experimental

4,4'-oxydiphthalic dianhydride (ODPA), and 4,4'-biphthalic dianhydride (BPDA) were used as received from TCI, Japan. For the monomer of the proton source, 3,3'-Bis(sulfopropoxy)-benzidine (BSPB) was synthesized according to previous reports.[14] The synthesis of the polymers, BSPB-ODPA (ASPI-3) and BSPB-BPDA (ASPI-4), were carried out according to the previous reports.[18] The obtained samples were checked by ^{1}H nuclear magnetic resonance (NMR), Fourier-transform infrared (FT-IR), and GPC measurements. No amic acid in the

polymer backbone was observed from ^{1}H NMR spectra. The weight average molecular weight and polydispersity of ASPI-3 and ASPI-4 were 4.4×10^5, 3.7 and 9.6×10^5, 3.8, respectively.

Proton conductivity was examined through impedance spectroscopy in the frequency range of 1 Hz and 10 MHz with an applied alternating potential of 50 mV using a Solartron 1260 frequency response analyzer equipped with a high-frequency Solartron 1296 dielectric interface. The relative humidity (RH) and temperature were established using a computer-controlled environmental test chamber (SH-221; Espec Corp). The conductivity measurements were performed at 298 K and various RH values. The pelletized samples were prepared as bulk samples. Porous gold electrodes were used for the both sizes of the pelletized surfaces. The conductivity (σ) of the bulk sample was estimated by the following relation,

$$\sigma = \frac{d}{RS} \quad (1)$$

where d is the distance between the gold electrodes, R is the resistance value obtained directly from the impedance measurement, and S is the area of electrode.

SAXS measurements in the bulk sample were performed on a Rigaku FR-E X-ray diffractometer with an R-AXIS IV two-dimensional (2D) detector and Cu Kα radiation (λ = 1.542 Å). A dry sample was placed in a capillary tube and was irradiated with the X-ray beam without further adjustments. For the measurements under the high-humidified condition, we placed both a portion of dry sample and a water droplet in the same capillary tube and then sealed it. After 7 days, we used the sealed capillary sample as the humidified bulk sample for SAXS measurements.

Grazing Incidence Small-angle X-ray Scattering (GISAXS) measurements were taken with the same machine of SAXS measurements. Thin film samples were prepared by spin coat and placed into a humidity-controlled cell with X-ray transparent polyester film (Lumirror) windows. Nitrogen carrier gas was used as received from the gas cylinder without further dehumidification to control the humidity. Voltage of 45 kV, current of 45 mA, and irradiation time of 1 h were applied with beam size of approximately 300 μm × 300 μm and camera length of 300 mm. X-ray scattering patterns were recorded on an imaging plate (Fujifilm Corp.). The incident angle was chosen as 0.20° – 0.22°. For 1D out-of-plane and in-plane profiles, the integrated regions were taken between -0.5° to +0.5° as 2 θ from the center (0°) and the width of 1° as 2θ, respectively.

FT-IR spectroscopy using an ATR method was carried out using an FT-IR spectrometer (Nicolet 6700; Thermo Fisher Scientific Inc.) equipped with deuterium triglycine sulfate (DTGS) detector to both square-shape samples of ASPI-3 and ASPI-4. The square-shape samples were prepared from the pelletized sample and cut it as a cubic-shape.

Results and discussion

Figure 1a shows RH dependence of proton conductivity for the thin film and bulk sample of ASPI-3. The proton conductivity between the thin film and bulk sample exhibited similar value in the low RH, however, the conductivity of the thin film was found to be much higher value than that of the bulk sample. The conductivity of thin film and bulk sample showed 6.1×10^{-2} S cm^{-1}[18] and 1.3×10^{-2} S cm^{-1} at RH = 95% and 298K, respectively. Figure 1b demonstrates the RH dependence of proton conductivity for the thin film and bulk sample of ASPI-4. The conductivity of the thin film was also higher than that of the bulk sample. The conductivity of

thin film and bulk sample showed 8.0×10^{-2} S cm^{-1}[18] and 1.6×10^{-2} S cm^{-1} at RH = 95% and 298K, respectively. To discuss the difference of the proton conductivity between thin films and bulk samples, SAXS measurements were carried out.

Figure 2 shows SAXS profiles of the bulk ASPI-3(a) and ASPI-4(b) under both dry and humidified conditions. In the dry condition, a weak scattering appeared at 4.6° (1.9 nm) and 5.3° (1.7 nm) for ASPI-3(a) and ASPI-4(b), respectively. After the humidified condition, both scatterings were enhanced and shifted to the smaller angle to 2.3°(3.9 nm) and 2.5° (3.6 nm) for ASPI-3(a) and ASPI-4(b), respectively. These trends for the peak shift and enhancement can be observed in another ASPI.[14] In the previous report, the ASPIs exhibits a lamellar structure parallel to the substrate surface in thin films and a non-oriented lamellar structure in bulk. The obtained peaks in bulk samples can be attributed as a non-oriented lamellar structure. Figure 3 shows GISAXS profiles for ASPI-3(a) and ASPI-4(b) thin films. The lamellar scatterings in both films were observed in the out-of-plane direction. The maximum lamellar distances are 3.08 and 2.94 nm, respectively. The observed lamellar distance of bulk ASPI-3 and ASPI-4 samples are larger than those of the thin films. Results suggest that the excess water was introduced to each bulk sample in the high RH region.

To check whether each bulk pelletized sample has a specific orientation or not, ATR spectra were carried out using square-shape samples. Figure 4a shows a schematic view of incident angles with X-, Y-, and Z-direction to samples. All spectra in each sample were found to be identical as shown in Figure 4b and 4c. The observed vibrational modes at 1380 cm^{-1} and 1500 cm^{-1} can be assigned to the C–N bonds of the main chain and to the phenyl C–C bonds, respectively. Adjacent vibrational modes at 1710 cm^{-1} and 1780 cm^{-1} correspond to the C=O

asymmetric and symmetric stretching vibrations of imide groups. Therefore both bulk ASPI-3 and ASPI-4 samples exhibit non-oriented lamellar structure.

In the dry state, proton conductivity did not exhibit an apparent difference between the thin films and bulk samples in both bulk ASPI-3 and ASPI-4 samples. The scattering intensity for both thin film and bulk sample with bent polymer backbone was found to be very weak in the dry state. The results suggests that the thin films and bulk in the dry state exhibit less molecular ordered structure and low proton conductivity. This suggestion is consistent with the previous report that the amorphous region contributes to the proton conduction in the dry state.[17] In the high RH region, the in-plane orientation of the polymer backbone along the substrate surface in the ASPI thin films can enhance the proton conductivity.[14-16] The molecular lamellar ordering was improved by water uptake in both thin films and bulk. On the other hand, the degree of backbone orientation in bulk samples should be less than that in thin films because of a lack of substrate. Moreover, the excess water uptake occurs in the bulk samples from the SAXS results. These two differences between thin films and bulk samples could affect the difference of the proton conductivity in the high RH region.

Summary

This work demonstrates that less orientation of the polymer backbone and excess water could decrease the proton conductivity. Results can extend the polymer design using the organized structure for the development of the highly proton-conductive polymers.

Acknowledgments

This work was supported in part by the Nanotechnology Platform Program (Molecule and Material Synthesis) of the Ministry of Education, Culture, Sports, Science and Technology (MEXT), Japan. This work was supported by JSPS KAKENHI Grant Number JP18K05257.

References

[1] T. D. Gierke, G. E. Munn, and F. C. Wilson. *J. Polym. Sci. Pol. Phys.*, **19**, 1687 (1981).

[2] W. Y. Hsu and T. D. Gierke. *J. Membr. Sci.*, **13**, 307 (1983).

[3] Y. Nagao. *Langmuir*, **33**, 12547 (2017).

[4] T. Kato, N. Mizoshita, and K. Kishimoto. *Angew. Chem. Int. Ed.*, **45**, 38 (2006).

[5] T. Kato, M. Yoshio, T. Ichikawa, B. Soberats, H. Ohno, and M. Funahashi. *Nat. Rev. Mater.*, **2**, 17001 (2017).

[6] T. Kato, J. Uchida, T. Ichikawa, and T. Sakamoto. *Angew. Chem. Int. Ed.*, **57**, 4355 (2018).

[7] Y. Chen, M. D. Lingwood, M. Goswami, B. E. Kidd, J. J. Hernandez, M. Rosenthal, D. A. Ivanov, J. Perlich, H. Zhang, X. Zhu, M. Möller, and L. A. Madsen. *J. Phys. Chem. B*, **118**, 3207 (2014).

[8] J. J. Hernandez, H. Zhang, Y. Chen, M. Rosenthal, M. D. Lingwood, M. Goswami, X. Zhu, M. Moeller, L. A. Madsen, and D. A. Ivanov. *Macromolecules*, **50**, 5392 (2017).

[9] I. Tonozuka, M. Yoshida, K. Kaneko, Y. Takeoka, and M. Rikukawa. *Polymer*, **52**, 6020 (2011).

[10] J. H. Lee, K. S. Han, J. S. Lee, A. S. Lee, S. K. Park, S. Y. Hong, J.-C. Lee, K. T. Mueller, S. M. Hong, and C. M. Koo. *Adv. Mater.*, **28**, 9301 (2016).

[11] J. Matsui, H. Miyata, Y. Hanaoka, and T. Miyashita. *ACS Appl. Mater. Inter.*, **3**, 1394 (2011).

[12] T. Sato, Y. Hayasaka, M. Mitsuishi, T. Miyashita, S. Nagano, and J. Matsui. *Langmuir*, **31**, 5174 (2015).

[13] T. Sato, M. Tsukamoto, S. Yamamoto, M. Mitsuishi, T. Miyashita, S. Nagano, and J. Matsui. *Langmuir*, **33**, 12897 (2017).

[14] K. Krishnan, H. Iwatsuki, M. Hara, S. Nagano, and Y. Nagao. *J. Mater. Chem. A*, **2**, 6895 (2014).

[15] K. Krishnan, T. Yamada, H. Iwatsuki, M. Hara, S. Nagano, K. Otsubo, O. Sakata, A. Fujiwara, H. Kitagawa, and Y. Nagao. *Electrochemistry*, **82**, 865 (2014).

[16] K. Krishnan, H. Iwatsuki, M. Hara, S. Nagano, and Y. Nagao. *J. Phys. Chem. C*, **119**, 21767 (2015).

[17] Y. Nagao, K. Krishnan, R. Goto, M. Hara, and S. Nagano. *Anal. Sci.*, **33**, 35 (2017).

[18] Y. Ono, R. Goto, M. Hara, S. Nagano, T. Abe, and Y. Nagao. *Macromolecules*, **51**, 3351 (2018).

[19] K. Takakura, Y. Ono, K. Suetsugu, M. Hara, S. Nagano, T. Abe, and Y. Nagao. *Polymer Journal*, (2018).

Scheme caption and Scheme

Scheme 1. Chemical structure of sulfonated polyimides. (a) ASPI-3 (b) ASPI-4.

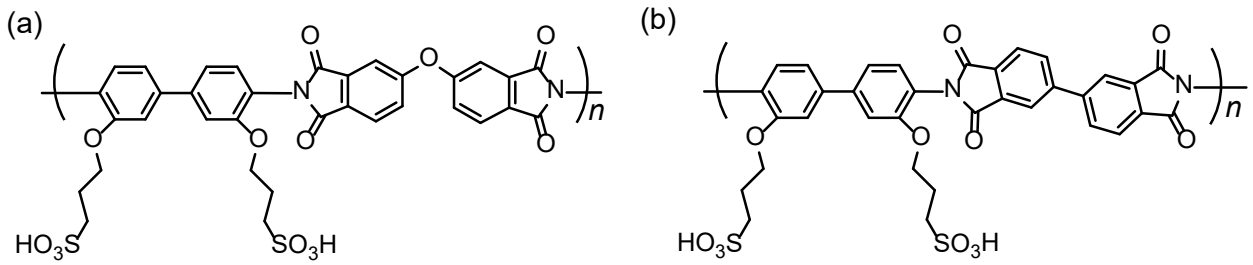

Scheme 1. (Y. Nagao et al.)

Figure captions

Figure 1. RH dependence of proton conductivity at 298 K. (a) Proton conductivity of thin film[18] and bulk in ASPI-3. (b) Proton conductivity of thin film[18] and bulk in ASPI-4.

Figure 2. SAXS profiles under dry and humidified condition in glass capillary. (a) bulk ASPI-3 (b) bulk ASPI-4.

Figure 3. GISAXS 2D profiles at RH = 95%. (a) ASPI-3 thin film (b) ASPI-4 thin film.

Figure 4. ATR spectra. (a) Schematic view of incident angles with X-, Y-, and Z-direction for ATR measurements to the square-shape samples. (b) bulk ASPI-3 (c) bulk ASPI-4.

Figures

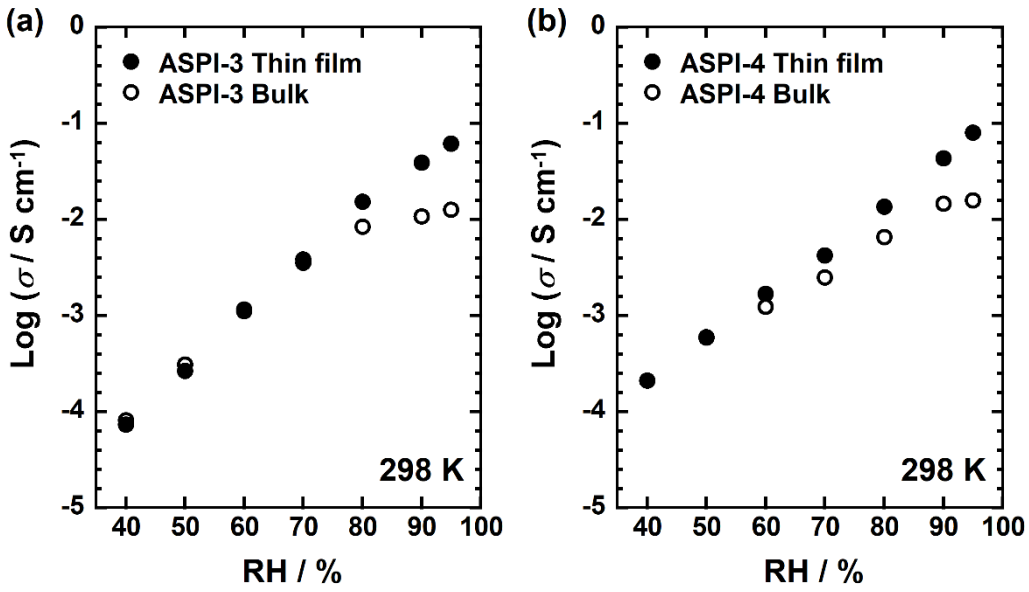

Figure 1. (Y. Nagao et al.)

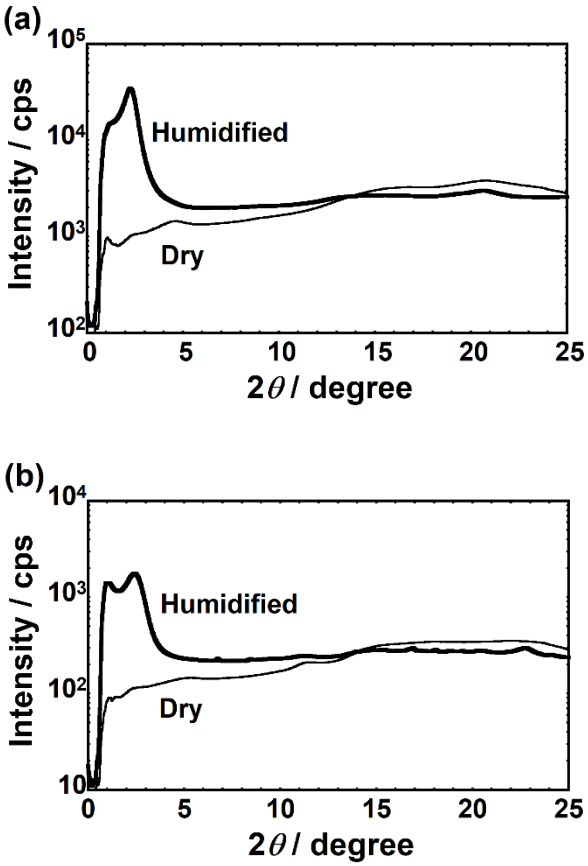

Figure 2. (Y. Nagao et al.)

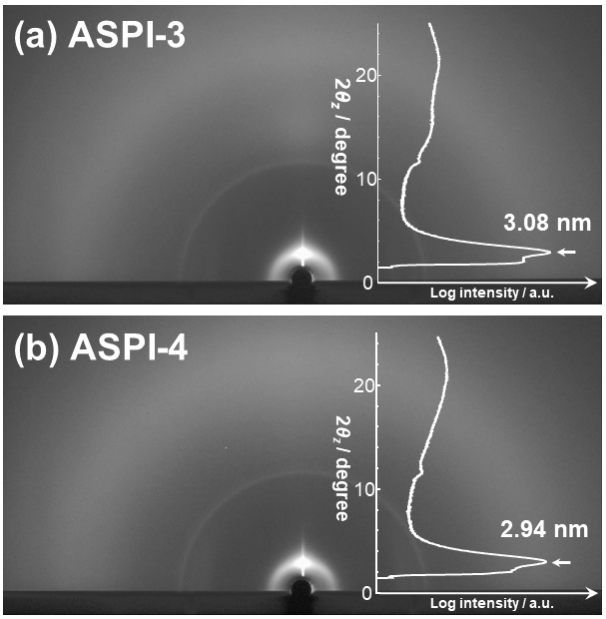

Figure 3. (Y. Nagao et al.)

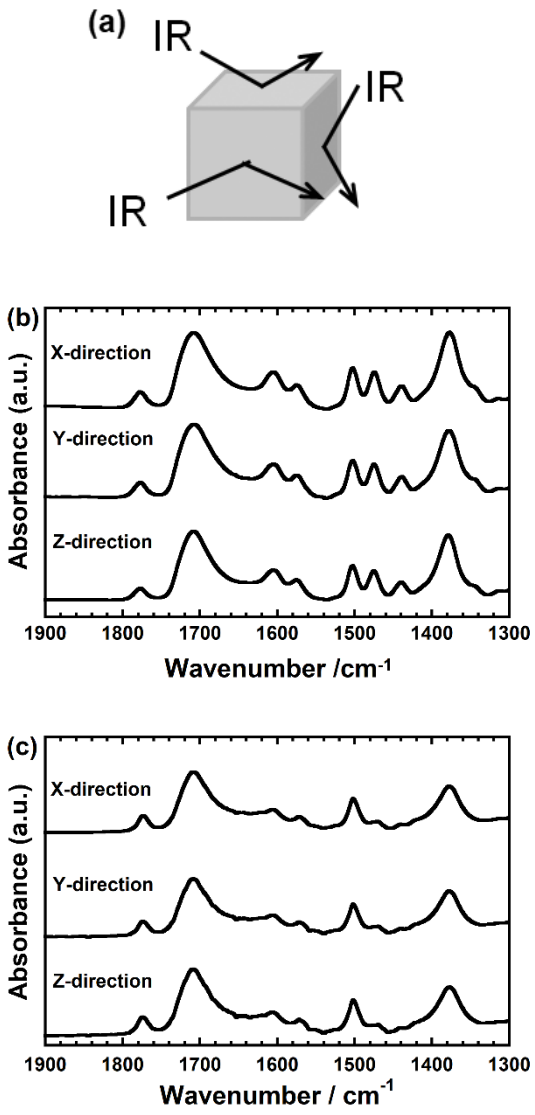

Figure 4. (Y. Nagao et al.)